The applications of InSAR technique for natural hazard detection in smart society

Journal of Physics: Conference Series **1572** (2020) 012067 doi:10.1088/1742-6596/1572/1/012067

The applications of InSAR technique for natural hazard detection in smart society

Jefriza[1], I M Yusoff[1], I A Abir[2], S Syahreza[3,4]*, M Rusdi[5], P Razi[6] and H Lateh[1]

[1]School of Distance Education, USM, Pulau Pinang, 11800, Malaysia
[2]School of Physics, 11800, Minden, Universiti Sains Malaysia, Malaysia
[3]Physics Department, Faculty of Mathematics and Natural Sciences, Syiah Kuala University, Banda Aceh 23111, Indonesia
[4]Tsunami and Disaster Mitigation Research Center (TDMRC), Unsyiah, Banda Aceh, 23233, Indonesia.
[5]Remote Sensing and Cartography Lab, Universitas Syiah Kuala, 23111 Darussalam, Aceh, Indonesia
[6]Physics Department, Faculty of Mathematics and Natural Sciences, Universitas Negeri Padang, Indonesia

*Corresponding author: ssyahreza@unsyiah.ac.id

Abstract. Synthetic Aperture Radar (SAR) is a potential application of remote sensing to geological and hydrometeorological hazards. This paper presents sustainability strategies for smart cities: the use of SAR Sentinel-1 for monitoring flood inundation and landslide hazards in Aceh Province, Indonesia. In this study, for flood detection, we attempt to uses Sentinel-1A (S-1A) in the same direction and acquisition through polarization of Vertical transmit and Vertical received (VV) – Vertical transmit and Horizontal received (VH) with a temporal baseline of 6 days. Those data were then analysed using the SNAP Toolbox. The results showed that the S-1A was successfully for detecting a flood inundation in which VH polarization is more sensitive than VV. For landslide monitoring, we apply multitemporal SAR images, where one of them is the Quasi-Persistent Scatterers (Q-PS) technique. Using ascending and descending orbit pass results in a better velocity map where both sides of the slope are detected due to the different sensor angle of both orbital passes. This technique has resulted in the undulating areas being monitored well and this will also fill the gap of layover and shadowing phenomena of the slant range SAR image. The Q-PS combinations were very effective to identify the deformation features associated with the land movement. For a smart city, natural hazards such as landslides and floods require continuous monitoring to ensure the potential as well as management and mitigation of natural hazards. Therefore, the InSAR technique is one of the effective ways for doing this strategy.

1. Introduction

Nowadays, as the world is getting more interconnected, large-scale urbanizationset a lot of pressure on the infrastructure. Public safety, healthcare, urban transportation, water, and energy management may arise with technologies that are relevant in particular areas. A smart society is a mandatory factor for building a smart city. Furthermore, if the city is in the hazard zone, such as landslide-prone areas, fault zone that can trigger an earthquake need an appropriate hazard detection and monitoring tool to minimize the loss of casualty and property. Detection and monitoring as the pre-hazard occurrence with

an appropriate tool are necessary. Interferometry Synthetic Aperture Radar (InSAR) with all the benefits can be the potential technology to detect such natural hazards which are not only in millimeter accuracy but also in wide areas. Moreover, InSAR is active remote sensing which can penetrate the cloud and work well both days and nights[1].

There is a successful application of the potential benefit of SAR images in natural disasters e.g., subsidence, earthquake, landslide, and flood [2-6]. Due to rapid change and large movement of the flood and earthquake, two of SAR images is enough for the study of the different surface water change surface deformation in the flood and earthquake, respectively. The images at least before and during the flood means that the peak of the highest of water level. The availability of those images has a higher possibility with the current ESA (European Space Bourne), S-1A, and S-1B Satellite SAR images. S-1A and S-1B work together in the different orbit pass can detect movement in 6 days (S1-A and S1-B revisit time interval)[7]. These active remote sensing satellite images the current of C-Band, with 5.6 cm wavelength, has the potential to monitor flood since the flood often occurs in the rainy season and cloud cover is high level. Cloud cover revealing quiet general limitations of the passive remote sensing. Moreover, active remote sensing can overcome the limitation of day, which is only available in passive remote sensing. However, to study landslide and subsidence, the availability of SAR images quantity has to be higher. The more images, the more precisely to achieve surface movement. Landslide and subsidence are the two cases that deformation could be minimal (e.g., 1 mm – 10 mm). The images stacking or time series of SAR images is mandatory for these movements. It is different from flood monitoring and earthquake mapping, with only use two SAR images.

Subsidence monitoring using InSAR application in the big city in Indonesia, such as Jakarta[3], [8] Bandar Lampung [9], Surabaya [10]. Meanwhile, the InSAR application has been researched in land deformation in Malang[11], Semarang[12], [13],Bandung [14]. InSAR application also shows great potential for deformation monitoring in the volcano areas in Indonesia, e.g. Mt. Raung [15], Mt. Merapi [16], Mt. Sinabung [17], Mt. Agung [18], and Rabaul Caldera at the next to Irian Jaya Province-Indonesian, Papua New Guinea[19].

Many research papers show subsidence monitoring, due to it often occurs in the city, e.g in Jakarta [3], [8]. The city usually located in flat areas which as an easier task to determine the location (height). However, undulating areas are more specific approaches to be used, since there are factors, such as active remote sensing only work in slant range, differ from passive remote sensing (use nadir when acquiring the images). Infrastructure can be a value-added to the active remote sensing image. Infrastructure such as building and road can be scattered points that can reflect the sensors. Reflected signal, they can determine the location and levelling infrastructure/building on the particular position on the Earth. InSAR has been useful to detect land subsidence, such as Lusi mud volcano, in Sidoarjo [20], land subsidence due to groundwater extraction [20] volcano [21]earthquake [22], landslide[23], peatland [24].

2. Study Area

Aceh Province, which is located in the north of Sumatra Island, has been a place for the laboratory of all-natural disasters since the most notable was an 8.9-moment magnitude earthquake and tsunami of 26 December 2004. Aceh often occurs natural disasters such as earthquakes, landslides, floods, and flash floods. Takengon is one of the districts where the landslides are more frequent. Takengon is a 100 km town from the westernmost edge with a population of less than 230,000. It is the capital of Central Aceh district with the topography of the area is hilly and in the mountains, Landslides are one of the disasters that often occur in this city, especially in those hilly and mountainous regions.The SAR satellite image for the application of landslide in Takengon City is shown in Figure 1.

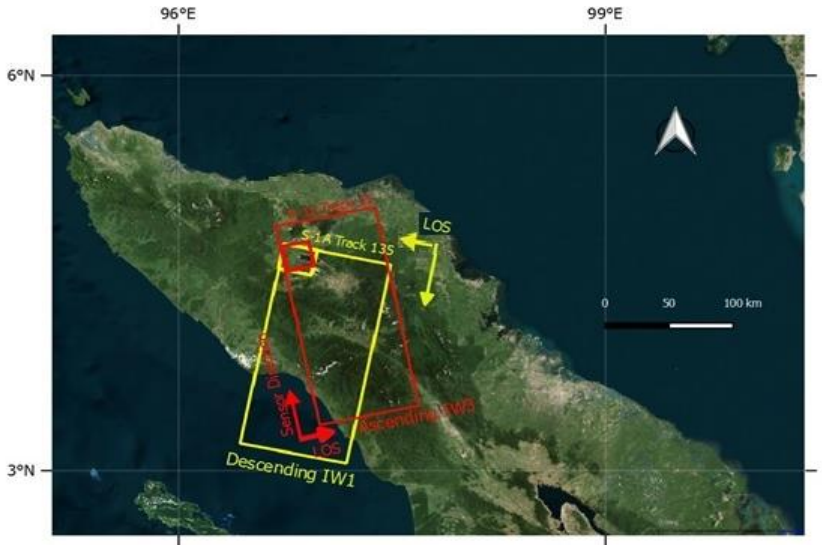

Figure 1. Sentinel-1A ascending (track 41-red) and descending (track 135-yellow) with the line of sight (Line of Sight and sensor direction). A small rectangle of red and yellow are the area of study is the Takengon city and a small part of Lut Tawar.

In 2018, at least 5 times flood destroy South of Aceh, Indonesia. To stay safe, people are evacuated to the nearest village even cross the neighbouring region. The issue is necessary since there is little information available in the site area. Since tropical regions, passive remote sensing image covers the present of the cloud and only can be obtained in the day, active remote sensing (synthetic aperture radar) overcome these restrictions due to great potentially time acquire even day or night. However, using active remote sensing such as Tandem of both radar sensors, Sentinel-1 is a value-added since its low revisit time 6 days and it is a value-added for flood monitoring. Some examples of successful applications of radar for flood monitoring[4], [25]The study area located at 2.295° N, 97.498° E to 3.239° N, 97.864° E South Aceh Regency, Aceh Province, Indonesia. This research focuses on Trumon, South Aceh, which was the most severe of this disaster. Figure 2 shows the location of the flood inundation monitoring.

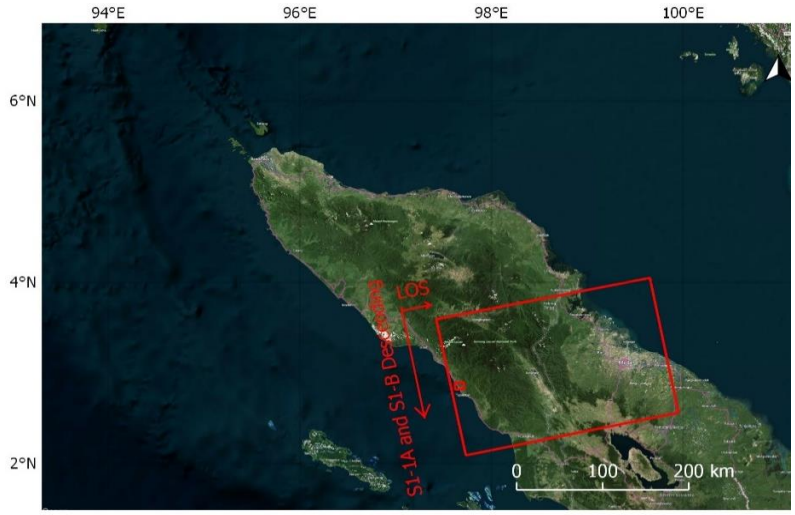

Figure 2. Large and small red rectangle are the footprint of S-1A and S-1B Descending Pass and Trumon Sub District Area (South Aceh), respectively.

3. Methodology

The study using two different methodologies, first the methodology for SAR satellite-based flood detection and second for deformation monitoring. The researchmethodology covers several major components: data collection, as above mentioned, we can detect flood by using only two ground range detected (GRD) Level 1.1 type of radar image. However, for landslide monitoring since the deformation is very slow (e.g. 1 mm -100 mm) (dependent on the radar sensors wavelength), more than two images have to be taken into account. Single Look Complex (SLC) Level 1.1 needs to be prepared.Two different methods can be used for flood detection and deformation monitoring. Flood detection used simple change detection of two GRD images, before and during the flood occurs. SNAP (Sentinel-1 Application Platform) toolbox is the default image processing in the Sentinel-1 for radar application. On the other hand, for deformation monitoring uses and advance of InSAR technique, which uses multi-temporal or stacking of the images. The most common option for advance InSAR techniques are Persistent Scatterer (PS), Small Baseline Subset (SBAS), and Quasi-PS. In this paper, PS and Q-PS are the technique will be used.

For S-1A datasets, using a new and originality of the SARPROZ software package is a promising tool for radar image processing. SARRPOZ with MatLab can detect and analyze the new and updated S-1A. The SARPROZ radar processing tool is developed by Perissin [26]. SARPROZ can analyse PS technique in urban [27], [28] and Quasi PS in natural mountainous terrain areas [29], [30]. SARPROZ offers Quasi-PS (Q-PS) with Minimum Spanning Tree (MST) graph that would be useful to detect and to monitor in deformation in a rural area. MST, which emphasizes in partial coherence target approach [26] works well in natural terrain. Q-PS is chosen as the radar image processing in the time series of the S-1A dataset. In order hand, SARPROZ also offers PS techniques. PS and Q-PS combinations then will be discussed.

3.1 Deformation monitoring

The main data sourcesuse an update radar image, S-1A Single Look Complex (SLC) image which is from the European Space Agency (ESA). Since the launch of S-1A satellite in April 2014, the available data on the site is between the late of December 2014 until continue up now. However, due to InSAR processing consuming time and limitation and specification of the computer, only between June 2018 until January 2019, radar image was downloaded and analyzed. 54 Ascending and 18 Descending of S-1A in Interferometric Wide Mode was described in detail in Table 1 and Table 2.

3.2 Flood detection

For the investigation flood area and damage analysis, the S-1A (C-Band) SAR data with Ground Range Detected (GRD) product format used. The mode of satellite data is Interferometric Wide (IW) which has a swath width area 250 km and has a dual-polarization (VV, VH) (Vertical Vertical, Vertical Horizontal). The GRD range and azimuth resolution are 20 x 22 m with pixel spacing 10x10 m [31]. This study using S-1A and S-1B GRD IW with the ESA-SNAPProcessor software with two image acquisition which is, before and during the flood occur. In this case, there are two data available, 11 and 17 December 2018 images. The first image acquisition (11-12-2018) is before the flood and the second (17-12-2018) is during the flood. The flood occurred on 13 December 2018 at 8.00 am until 18 December 2018. Because of the flood stay up until the next days, therefore these acquiring date of S-1A and S-1B are compatible for the site area since the Sentinel-1 time acquiring is at the morning11.42 - 11.43 local time. It means Sentinel-1 captured the flood event and suitable for this research. However, according to local government (BPBD-Badan Penanggulangan Bencana Daerah), the peak of water inundated on 14 December 2018, the flood still appeared on 17 December 2018. Table 3 shows the S-1A data.

Table 1. Availability of S-1A 54, track 41 Ascending SLC IW3 VV Polarization

No.	Date	Baseline Perp.(m)	Orbit No.	Temporal (days)	Track No.
1	2017-03-26	28.5042	15863	0	41
2	2017-04-07	76.5985	16038	12	41
3	2017-04-19	83.1599	16213	12	41
4	2017-05-01	53.121	16388	12	41
5	2017-05-13	94.4696	16563	12	41
6	2017-05-25	1.5656	16738	12	41
7	2017-06-06	77.132	16913	12	41
8	2017-06-18	49.8635	17088	12	41
9	2017-06-30	28.9765	17263	12	41
10	2017-07-12	11.269	17438	12	41
11	2017-07-24	3.2698	17613	12	41
12	2017-08-05	58.6162	17788	12	41
13	2017-08-17	59.8042	17963	12	41
14	2017-08-29	64.3413	18138	12	41
15	2017-09-10	49.6867	18313	12	41
16	2017-09-22	31.4121	18488	12	41
17	2017-10-04	8.7788	18663	12	41
18	2017-10-16	28.8499	18838	12	41
19	2017-10-28	88.7408	19013	12	41
20	2017-11-09	12.7772	19188	12	41
21	2017-11-21	56.1721	19363	12	41
22	2017-12-03	-36.3189	19538	12	41
23	2017-12-15	-17.0975	19713	12	41
24	2017-12-27	-44.6924	19888	12	41
25	2018-01-08	20.521	20063	12	41
26	2018-01-20	60.3347	20238	12	41
27	2018-02-01	7.136	20413	12	41
28	2018-02-13	42.7673	20588	12	41
29	2018-02-25	6.8055	20763	12	41
	~~**2018-03-09**~~	~~**No DATA**~~	-		-
30	2018-03-21	-51.0377	21113	24	41
31	2018-04-02	0 (Master Scene)	21288	12	41
32	2018-04-14	55.6747	21463	12	41
33	2018-04-26	29.132	21638	12	41
34	2018-05-08	31.1311	21813	12	41
35	2018-05-20	32.2241	21988	12	41
36	2018-06-01	-17.4774	22163	12	41
37	2018-06-13	43.2689	22338	12	41
38	2018-06-25	41.5774	22513	12	41
39	2018-07-07	-15.8673	22688	12	41
40	2018-07-19	44.4772	22863	12	41
41	2018-07-31	-27.5516	23038	12	41
42	2018-08-12	2.7976	23213	12	41
43	2018-08-24	4.2438	23388	12	41
44	2018-09-05	102.0835	23563	12	41
45	2018-09-17	64.9604	23738	12	41
46	2018-09-29	36.452	23913	12	41
47	2018-10-11	44.878	24088	12	41
48	2018-10-23	2.5903	24263	12	41
49	2018-11-04	12.2972	24438	12	41
50	2018-11-16	55.6579	24613	12	41
51	2018-11-28	-11.611	24788	12	41
52	2018-12-10	13.3661	24963	12	41

53	2018-12-22	3.9665	25135	12	41
54	2019-01-03	0.26617	25313	12	41

Table 2. Availability of S-1A 18 images Descending, track 135 SLC IW1 VV Polarization

No.	Date	Baseline Perp.(m)	Orbit No.	Temporal (days)	Track No.
1	2018-06-19	34.5473	22432	0	135
2	2018-07-01	42.8466	22607	12	135
3	2018-07-13	6.2557	22782	12	135
4	2018-07-25	10.2937	22957	12	135
5	2018-08-06	-13.1216	23132	12	135
6	2018-08-18	-20.7337	23307	12	135
7	2018-08-30	-49.3395	23482	12	135
8	2018-09-11	13.889	23657	12	135
9	2018-09-23	0 (Master scene)	23832	12	135
10	2018-10-05	18.6327	24007	12	135
11	2018-10-17	-86.3434	24182	12	135
12	2018-10-29	-73.2204	24357	12	135
13	2018-11-10	-55.3373	24532	12	135
14	2018-11-22	-6.5605	24707	12	135
15	2018-12-04	-58.02	24882	12	135
16	2018-12-16	43.1581	25057	12	135
17	2018-12-28	-72.2274	25232	12	135
18	2019-01-09	-14.518	25407	12	135

Table 3. Satellite S-1A with dual-polarization VV, VH and azimuth range resolution 20 x 22 m.

Satellite Data	Pass Direction	Time	Track	Date (Nov 2018)	Orbit
Sentinel-1A	Descending	11.42 am	143	11	13994
Sentinel-1B				17	25065

Flood detection can be analysed by its coefficient of backscatter (Sigma 0), which has a low value than others because the satellite signal reflected away from the sensor then the area looks dark (black) in SAR images. The processing flow by using ESA SNAP Processing Tool [35] is shown in Figure 10.

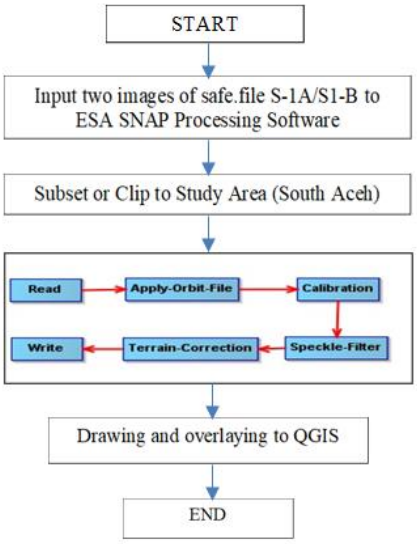

Figure 3. A flowchart of methodology with using ESA SNAP and QGIS

For flood detection, we used before and during flood images to compare water and land area. To decide the value threshold, statistical analysis was applied for selecting the water area. The water class area, which has a minimum of backscatter than the land class area. In this case, we used before the flood, water in the river (2°49'57" N, 97°37'01" E or Sample 6448 12837 Line) was detected value of 0.0591 for VH polarization. Then the threshold we selected was 0.0591. It means the coefficient value > 0.0591 corresponds to the land area. When the time of satellite acquisition is more than 3 days from the peak of flooding (14 to 17 December 2018) then some field less identified. However, the flood is still occurring. Based on the amplitude value of VV and VH, the area of the study depicted in Figure 4.

Figure 4. Satellite view of the study area, Trumon, South of Aceh

4. Results and Discussion

4.1 Deformation

PS with a "one-star" graph of the two 54 and 18 ascending and descending datasets are shown in Figure 5 and Figure 7, respectively. The master image with the red dot and with the center of the star graph is shown in Figures 7 and 8. The master image is selected by manually based on the interpretation with no rain at that acquisition time.

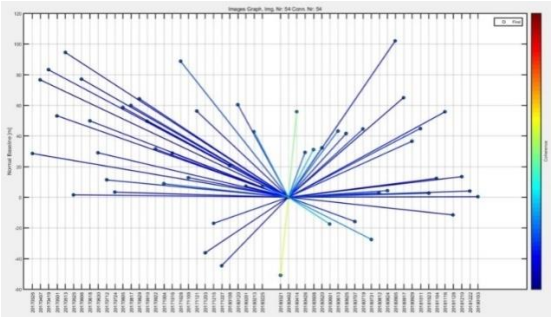

Figure 5. 54 images in ascending andin (PS) One Star Graph

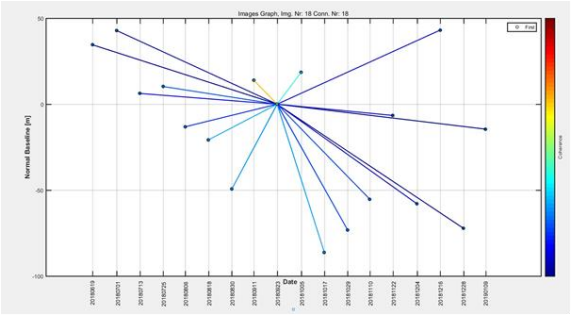

Figure 6. 18 images in descending in (PS) One Star Graph

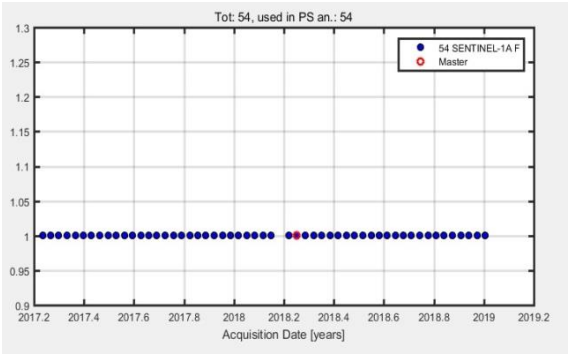

Figure 7. Time series of 54 ascending SLC images

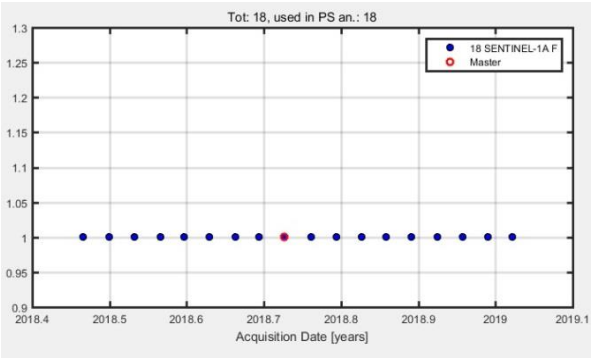

Figure 8. Time series of 18 descending SLC images (below)

Figure 9 shows the velocity deformation of the PS result with S-1A in the LOS direction. The deformation appears clearly in the city or urban area (Takengon city), whereas many backscattered points such as building and other man-made infrastructures. Meanwhile, in the Northern left corner of the map (white circle) also appears the occurrence of the deformation in the natural terrain. Figure 10 shows the cumulative displacement of the natural terrain southern part of the Lut Tawar Lake. This natural slope is very important to study since the occurrence of the displacement of the ground is higher. Moreover, the slope is beside the main road of Lut Tawar Lake that can dangerous the road user and surrounding village. There is 6 points ID that shows the high value of cumulative displacement (Figure 8). Figure 11 shows the graph of displacement trend of point ID 6 and ID 17. Where other points which are ID 19, 20, 24, and 30 show similar deformation with ID 6.

Figure 12 shows the Line of Sight (LOS) direction in the S-1A Descending Orbit pass. Ground profile in this case natural terrain in West direction shows a good correlation to LOS direction satellite. In Descending orbit pass, PS density higher at slope which is facing to the West, because the satellite crosses the sloping topography. It shows an agreement to[33]that stated descending geometry is better for slopes oriented to the West. The target point (ID 6) with low coherence 0.5 can be monitored with the Quasi-PS technique with high movement capability in the natural terrain area. The off-nadir angle of S-1A in descending orbit pass on the part Interferometric Width 1 (IW1) is typically in the range 26.53° – 32.48°, then in shadow area cannot be penetrated by the satellite signal [31].

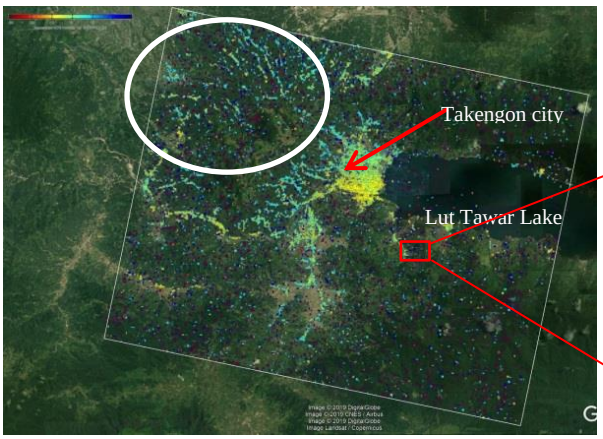

Figure 9. Velocity of S-1A Descending in LOS (line of sight) direction with number of points detected 16423

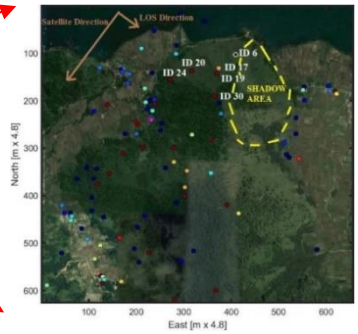

Figure 10. Cumulative displacement of natural terrain in Southern part of Lake

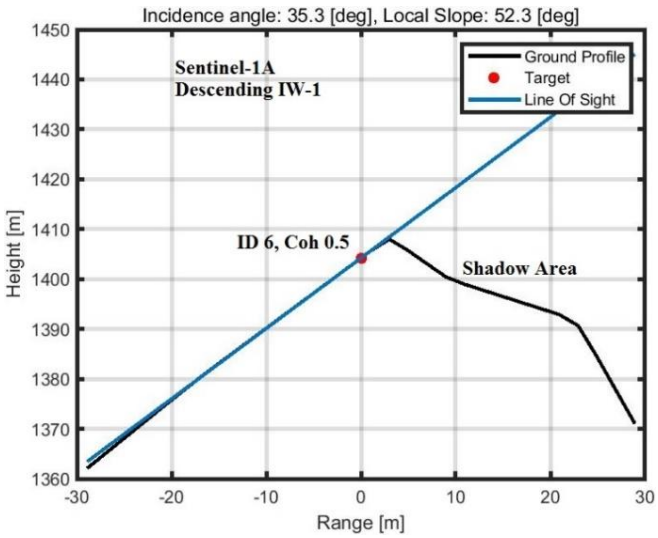

Figure 11. Velocity of Sentinel-1A Descending in LOS (line of sight) direction with number of points detected 16423

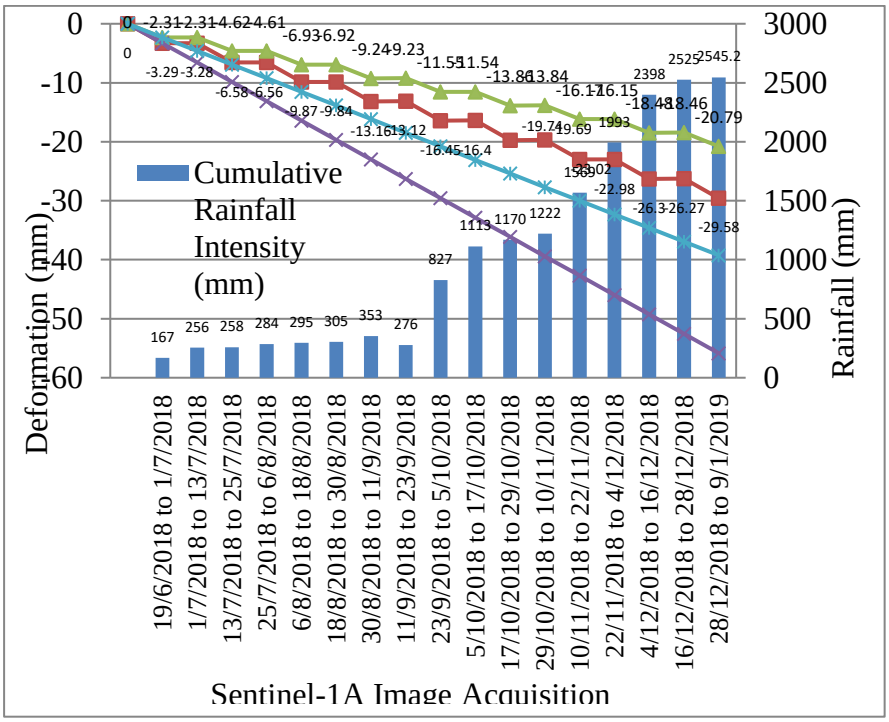

Figure 12. Cumulative displacement of natural terrain in Southern part of Lut Tawar Lake

4.2 Floods

The results present the potential for detecting flood events using S-1A GRD images with the InSAR technique. The differences VH polarizations either before and during a flood are shown in Figures 13 and 14. The monitoring over the Southern and Northern parts of the river very clearly showed the dark areas, especially in the inundated area. However, in the Northern part of the river, although the water was still inundated, yet less dark than the Southern and Eastern parts. On the other hand, Figure 15 and

16 in the VV polarization perspective, in which similar to VH polarization. In the Southern and northern part of the river, VV polarization of the inundated area shows darker when compares before the flood. In the center up to the Southern part, water inundated most of the area. However, in this study, VH polarization has more potential to identify flood inundation than VV polarization.

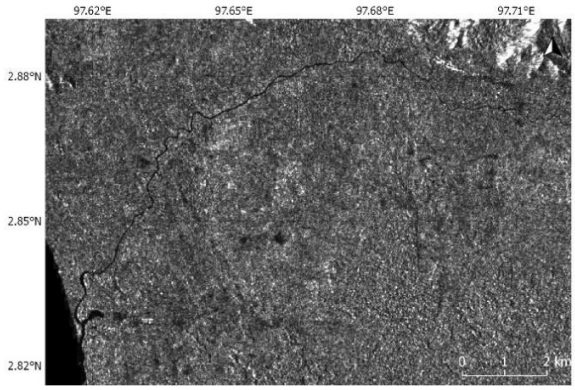

Figure 13. VH Before Flood

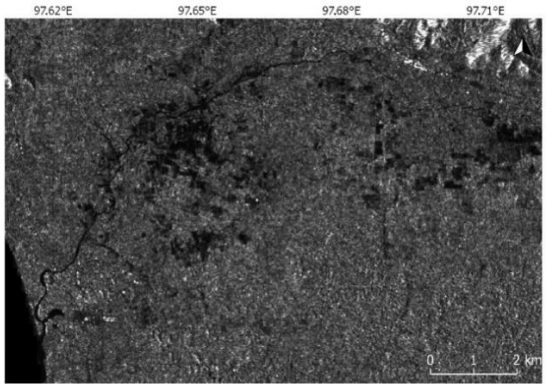

Figure 14. VH During Flood

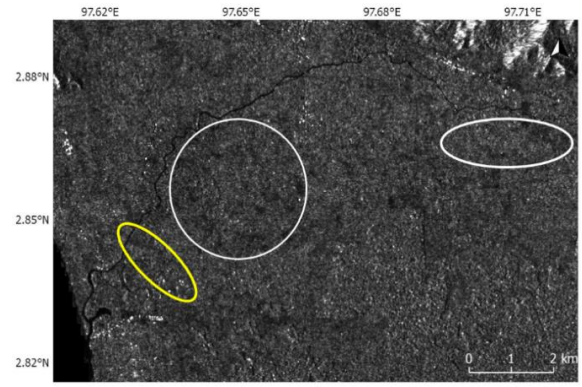

Figure 15. VV Before Flood

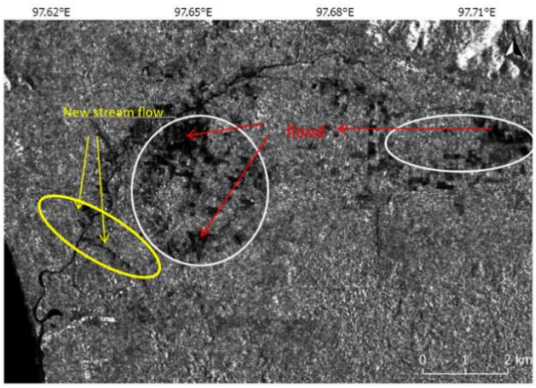

Figure 16. VV During Flood

5. Conclusion

Based on the two examples of natural hazards, landslide deformation, and flood detection using InSAR techniques, concluded that radar image could be the potential application for mapping such evidence. Nowadays, with all the capabilities of InSAR techniques, radar images show a positive trend to use and to interpret natural hazard in the smart city. For smart society, radar processing could be useful to map flooding in wide areas without overlay immediate government activity such as, for evacuation, medical treatment, and blanket and tend and food distribution to the victims and refugees. In other words, flood mapping with remote sensing is not disturbing any other agencies. For landslide monitoring using InSAR techniques could also benefit the society since the InSAR techniques can detect very small movement (e.g. 1-10 cm) as a pre-landslide movement. It gives a warning sign before real landslide occurs. Landslide monitoring with InSAR shows a large scale (e.g. in district or sub-district) could be mapped continuously.

6. References

[1] Z Li, W Tim, A Hooper, P Crippa, P Gonzalez, R Walters, J Elliott, J Ebmeier, S Hatton and Emma Towards InSAR everywhere, all the time, with Sentinel-1 *Int. Arch. Photogramm. Remote Sens. Spat. Inf. Sci. - ISPRS Arch.* vol. 41, no. July, pp. 763–766, 2016.

[2] Jefriza, H Lateh and S Syahreza, "Co-Seismic Deformation Using InSAR Sentinel-1A : Case Stu dy of the 6 . 5 Mw Pidie Jaya , Aceh , Earthquake," *Int. J. Geol. Enviromental Eng. World Acad. Sci. Eng. Technol.*, vol. 4, no. 4, p. 69671, 2017.

[3] J Widodo, H Arie, A Sulaiman, P Razi, Yohandri, D Perissin, H Kuze and J T Sri Sumantyo, "Land subsidence rate analysis of Jakarta Metropolitan Region based on D-InSAR processing of Sentinel data C-Band frequency," *J. Phys. Conf. Ser.*, vol. 1185, no. 1, 2019.

[4] P Razi, J T S Sumantyo, F Febriany, M Nasucha, and J Aminuddin, "Interferometry Synthetic Aperture Radar (InSAR) Application for Flood Area Detection Observed by Sentinel 1A," in *Progress in Electromagnetics Research Symposium PIERS*, 2018, pp. 905–909.

[5] S Syahreza, Fadhli, A Saepuloh, Jefriza and H Lateh, "Combining the Sentinel-1A/B DinSAR Interferometry to Detect Deformation Associated with Pidie Jaya Earthquake," *J. Phys. Conf. Ser.*, vol. 1120, no. 1, p. 012021, Nov. 2018.

[6] S Syahreza, H H Siddieq, A Saepuloh and I Mailano, "Deformation monitoring of Pidie Jaya earthquake using pairwise logic of multitemporal Sentinel-1 SAR data," *AIP Conf. Proc.*, vol. 1987, 2018.

[7] T Carlà, P Farina, E Intrieri, H Ketizmen and N Casagli, "Integration of ground-based radar and satellite InSAR data for the analysis of an unexpected slope failure in an open-pit mine," *Eng. Geol.*, vol. 235, no. September 2017, pp. 39–52, 2018.

[8] Agustan, A Sulaiman and T Ito, "Measuring Deformation in Jakarta through Long Term Synthetic Aperture Radar (SAR) Data Analysis," *IOP Conf. Ser. Earth Environ. Sci.*, vol. 47, no. 1, 2016.

[9] A Zaenudin, I G B Darmawan, Armijon, S Minardi and N Haerudin, "Land subsidence analysis in Bandar Lampung City based on InSAR," *J. Phys. Conf. Ser.*, vol. 1080, no. 1, 2018.

[10] M Mochammad and A Saepuloh, "Analyses of surface deformation with SBAR InSAR method and its relationship with aquifer occurrence in Surabaya City, East Java, Indonesia," *IOP Conf. Ser. Earth Environ. Sci.*, vol. 71, no. 1, 2017.

[11] D Sudiana, Rokhmatuloh, M Rizkinia, Ardiansyah R A, B Setiadi, L Bayuaji and J T Sri Sumantyo, "Analysis of Land Deformation on Slope Area using PS InSAR. Case Study: Malang Area," *IOP Conf. Ser. Earth Environ. Sci.*, vol. 19, no. February, p. 012011, 2014.

[12] R Azeriansyah, Y Prasetyo and B D Yuwono, "Land Subsidence Monitoring in Semarang and Demak Coastal Areas 2016-2017 Using Persistent Scatterer Interferometric Synthetic Aperture Radar," *IOP Conf. Ser. Earth Environ. Sci.*, vol. 313, p. 012040, Aug. 2019.

[13] Y Prasetyo, H S Firdaus and Diyanah, "Land Subsidence Of Semarang City Using Permanent Scatterer Interferometric Synthetic Aperture Radar (Ps-Insar) Method In Sentinel 1a Between 2014-2017," *IOP Conf. Ser. Earth Environ. Sci.*, vol. 313, p. 012044, Aug. 2019.

[14] Y Maghsoudi, F van der Meer, C Hecker, D Perissin and A Saepuloh, "Using PS-InSAR to detect surface deformation in geothermal areas of West Java in Indonesia," *Int. J. Appl. Earth Obs. Geoinf.*, vol. 64, no. March 2017, pp. 386–396, Feb. 2018.

[15] A P Arbad, W Takeuchi, A Ardy and R A Ashari, "Observing Deformation at Mt. Raung East Java Based on PALSAR-2 Imagery by Using Interferometric SAR," *IOP Conf. Ser. Earth Environ. Sci.*, vol. 47, no. 1, p. 12021, 2016.

[16] A Pamungkas, T Osawa and I Adnyana, "Monitoring of Merapi Volcano Deformation Using Interferometry Synthetic Aperture Radar (InSAR) Technique," *J. Environ.*, vol. 1, no. 1, pp. 1–9, 2014.

[17] C W Lee, Z Lu, J W Kim, and S K Lee, "Volcanic activity analysis of Mt. Sinabung in Indonesia using InSAR and GIS techniques," *Int. Geosci. Remote Sens. Symp.*, vol. 2015-Novem, no. 1, pp. 4793–4796, 2015.

[18] J Lingyun, W Qingliang, and Q Shanlan, "Present-day deformation of Agung volcano, Indonesia, as determined using SBAS-InSAR," *Geod. Geodyn.*, vol. 4, no. 3, pp. 65–70, Aug. 2013.
[19] M C Garthwaite, V L Miller, S Saunders, M M Parks, G Hu and A L Parker, "A simplified approach to operational InSAR monitoring of volcano deformation in low-and middle-income countries: Case study of Rabaul Caldera, Papua New Guinea," *Front. Earth Sci.*, vol. 6, no. January, 2019.
[20] E Chaussard, F Amelung, H Abidin, and S H Hong, "Sinking cities in Indonesia: ALOS PALSAR detects rapid subsidence due to groundwater and gas extraction," *Remote Sens. Environ.*, vol. 128, pp. 150–161, 2013.
[21] A Hooper, D Bekaert, K Spaans and M Arikan, "Recent advances in SAR interferometry time series analysis for measuring crustal deformation," *Tectonophysics*, vol. 514–517, pp. 1–13, 2012.
[22] K Dai, Z Li, R Tomás, G Liu, B Yu, X Wang, H Cheng and J Chen, "Monitoring activity at the Daguangbao mega-landslide (China) using Sentinel-1 TOPS time series interferometry," *Remote Sens. Environ.*, vol. 186, pp. 501–513, 2016.
[23] E Intrieri, R Federico, A Fumagalli, P Lu, S Del Conte, P Farina, J Allievi and A Ferretti, "The Maoxian landslide as seen from space: detecting precursors of failure with Sentinel-1 data," *Landslides*, vol. 15, no. 1, pp. 123–133, 2018.
[24] Z. Zhou, "The applications of InSAR time series analysis for monitoring long-term surface change in peatlands," 2013.
[25] A Refice, C Domenico, G Pasquariello, A Annarita, F Bovenga, R Nutricato and F Lovergine, "SAR and InSAR for Flood Monitoring : Examples With COSMO-SkyMed Data," vol. 7, no. 7, pp. 2711–2722, 2014.
[26] D Perissin and T Wang, "Repeat-Pass SAR Interferometry With Partially Coherent Targets," *IEEE Trans. Geosci. Remote Sens.*, vol. 50, no. 1, pp. 271–280, Jan. 2012.
[27] D Perissin, Z Wang and T Wang, "The SARPROZ InSAR tool for urban subsidence/manmade structure stability monitoring in China," in *In Proceeding of 34th ISRSE 10-15 April 2011*, 2011.
[28] D Perissin and A Ferretti, "Urban-target recognition by means of repeated spaceborne SAR images," *IEEE Trans. Geosci. Remote Sens.*, vol. 45, no. 12, pp. 4043–4058, 2007.
[29] D Perissin, R Piantanida, D Piccagli and F Rocca, "Landslide in Dossena (BG): comparison between interferometric techniques," *Biogeosar*, vol. 9, no. May 2014, pp. 1–7, 2007.
[30] P Razi, J T S Sumantyo, D Perissin and H Kuze, "Long-Term Land Deformation Monitoring Using Quasi-Persistent Scatterer (Q-PS) Technique Observed by Sentinel-1A: Case Study Kelok Sembilan," *Adv. Remote Sens.*, vol. 07, no. 04, pp. 277–289, 2018.
[31] ESA User Guide, "Interferometric Wide Swath," *Online*, 2019. [Online]. Available: https://sentinel.esa.int/web/sentinel/user-guides/sentinel-1-sar/acquisition-modes/interferometric-wide-swath.
[32] Sentinel-1 Tutorials, "SNAP Proccessing and Tutorials," 2016. [Online]. Available: http://step.esa.int/. [Accessed: 11-Dec-2016].
[33] ESA, *Sentinel-1 User Handbook*. 2013.

Acknowledgments
The authors wish to thank the European Space Agency (ESA) for the Sentinel-1A SLC images and SARPROZ for providing processing tool for Sentinel-1 images. Jefriza's work was supported by BPSDM (Badan Pemberdayaan Sumber Daya Manusia Aceh) scholarship.